Interfacial flow around a pusher bacterium

Supporing Information

Jiayi Deng, Mehdi Molaei, Nicholas G. Chisholm and Kathleen J. Stebe

1 Estimating Bacteria trapping angle

We use Bayesian inference to estimate trapping angle of bacteria at the interface based on their measured apparent aspect ratio, γ considering its probability distribution, $P_\gamma(\gamma)$, and also probability distribution of bacteria body aspect ratio $P_{\gamma_b}(\gamma_b)$. We use spherocylinder model for bacterial body shape to determine trapping angle from known body and apparent aspect ratio, $\cos\theta = (\gamma-1)/(\gamma_b-1)$. To determine trapping angle with known probability distribution of body aspect ratio $P_{\gamma_b}(\gamma_b)$ and measured γ we use

$$\cos(\theta) = (\gamma-1)\int \frac{P(\gamma_b|\gamma)}{\gamma_b-1} d\gamma_b \tag{S1}$$

Where $P(\gamma_b|\gamma)$ is the probability distribution of γ_b when γ is observed; this quantity is determined using Bayesian inference,

$$P(\gamma_b|\gamma) = \frac{P(\gamma|\gamma_b)P_{\gamma_b}(\gamma_b)}{P_\gamma(\gamma)}. \tag{S2}$$

$P(\gamma|\gamma_b)$ is the probability distribution of the γ if the body aspect ratio measured to be γ_b. Since γ is always smaller than γ_b we assume $P(\gamma|\gamma_b) = P_\gamma(\gamma)/F_\gamma(\gamma_b)$, where F_γ is the cumulative distribution of the apparent aspect ratio, $F_\gamma(\gamma_b) = \int_1^{\gamma_b} P(\gamma)d\gamma$. These equations are evaluated numerically to determine the function that maps apparent aspect ratios to the trapping angles (shown in Figure. S1). For compression we compare this mapping function obtained using the median value of γ_b

$$\cos(\theta) = \begin{cases} \dfrac{\gamma-1}{\langle\gamma_b\rangle-1} & \gamma < \langle\gamma_b\rangle \\ 1 & \text{otherwise} \end{cases} \tag{S3}$$

The resulting distribution of estimated trapping angles is shown in Figure. S2.

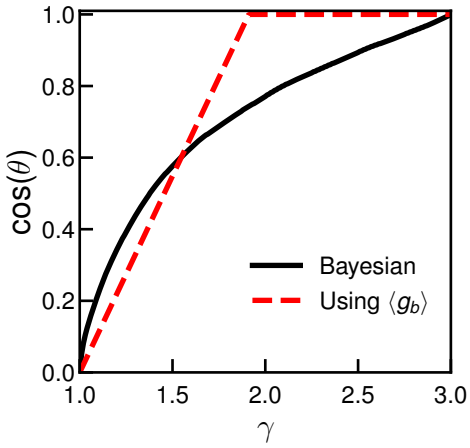

Figure S1: Trapping angle of bacteria based on apparent aspect ratio. Black line indicates the mapping function obtained by numerically evaluating equation S1. Red line indicates mapping function obtained from equation S3 shown for comparison.

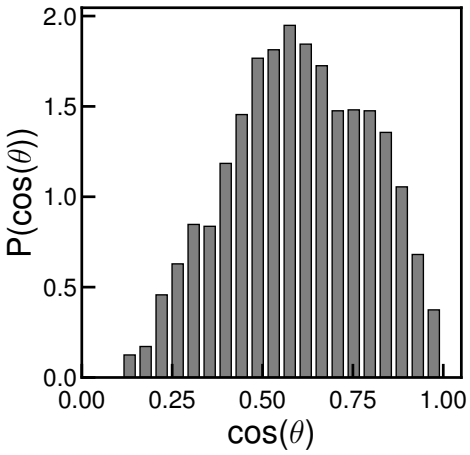

Figure S2: Distribution of estimated trapping angle. The trapping angle of pusher bacteria at fluid interfaces are calculated using Bayesian inference, equation S1.

2 Interfacial flow fields

As mentioned in the main text, Chisholm and Stebe [2021] give a detailed derivation of the far-field flow modes due to a self-propelled object adhered to an interface assuming negligible fluid inertia. Here, we focus specifically on the parts of this model that predict the interfacial flow field observed in experiment. For a free swimming bacterium with no external forces or torques, the far-field flow is predicted to be

$$u_i(\boldsymbol{r}) = S^{\shortparallel}_{\alpha\beta}\Delta^{\shortparallel}_{i\alpha\beta}(\boldsymbol{r}) + \frac{1}{2}A_\alpha\Delta^{\ddagger}_{i\alpha}(\boldsymbol{r}) + \frac{1}{2}B_\beta Q_{i\alpha}(\boldsymbol{r}), \tag{S4}$$

where $\boldsymbol{r}$ is the position vector, The analytical form of the flow field generated by the $\boldsymbol{S}$ mode on the interfacial plane is given by

$$u_i^S(\boldsymbol{r}) = \frac{S_{jk}}{4\pi\bar{\mu}}\left[\frac{3r_ir_jr_k}{r^5} - \frac{r_i\delta_{jk} + r_j\delta_{ik}}{r^3}\right] = \frac{1}{4\pi\bar{\mu}}\left[\frac{3(\boldsymbol{r}\cdot\boldsymbol{S}\cdot\boldsymbol{r})\boldsymbol{r}}{r^5} - \frac{(\operatorname{tr}\boldsymbol{S})\boldsymbol{r} + \boldsymbol{S}\cdot\boldsymbol{r}}{r^3}\right] \tag{S5}$$

where $\boldsymbol{S}$ is a second-order tensor whose components have units of force time length, $\boldsymbol{r} = \boldsymbol{x}' - \boldsymbol{x}'_h$ is the position vector relative to the hydrodynamic origin $\boldsymbol{x}'_h$ and $r = \|\boldsymbol{r}\|$. The tensor $\boldsymbol{S}$, which is denoted $\boldsymbol{S}^{\shortparallel}$ in Chisholm and Stebe [2021], has the property of being traceless and symmetric, i.e., $\operatorname{tr}\boldsymbol{S} = 0$ and $\boldsymbol{S} = \boldsymbol{S}^\top$, respectively, where $^\top$ denotes the transpose. It therefore admits the eigendecomposition given by

$$\boldsymbol{S} = S\left(\boldsymbol{q}^S\boldsymbol{q}^S - \frac{1}{2}\boldsymbol{I}\right), \tag{S6}$$

where $\boldsymbol{q}^S$ is the normalized eigenvector of $\boldsymbol{S}$ associated with the eigenvalue $\lambda_1^S = S/2$. The other eigenvector is perpendicular to $\boldsymbol{q}^S$ and is associated with the eigenvalue $\lambda_2^S = -\lambda_1^S = -S/2$. The scalar coefficient S in (S6) is the nuclear norm of $\boldsymbol{S}$, given by $S = |\lambda_1^S| + |\lambda_2^S|$, and measures the "strength" of the $\boldsymbol{S}$ mode.

Note that while (S6) expresses $\boldsymbol{S}$ in terms of just a single vector $\sqrt{S}\boldsymbol{q}^S$, the $\boldsymbol{S}$ mode (S7) does not assume that the the bacteria have an axis of symmetry. From (S7), it is apparent that the unit vector $\boldsymbol{q}^S$ is associated with the spatial orientation of the $\boldsymbol{S}$ mode. We therefore introduce the $\boldsymbol{S}$-mode orientation angle ϕ^S relative to the *vertical* axis, which is given by $\boldsymbol{q}^S = \langle -\sin\phi^S, \cos\phi^S\rangle$.

Using (S6), (S5) may be alternatively expressed as

$$\boldsymbol{u}^S(\boldsymbol{r}) = \frac{S}{4\pi\bar{\mu}}\left[\frac{3(\boldsymbol{q}^S\cdot\boldsymbol{r})^2\boldsymbol{r}}{r^5} - \frac{(\boldsymbol{q}^S\cdot\boldsymbol{r})\boldsymbol{q}^S + \boldsymbol{r}}{r^3}\right]. \tag{S7}$$

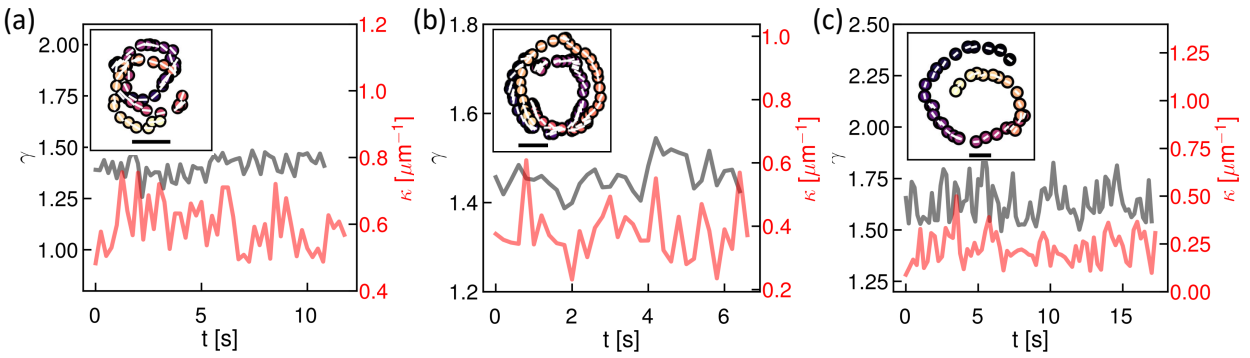

Figure S3: Fixed aspect ratio of the cell body and persistent curly motion of bacteria indicate contact line pinning and interfacial trapping. Three example trajectories of bacteria are shown in (a-c). Instantaneous swimming curvature versus time (red line). Instantaneous aspect ratio of the cell body (grey line). Inset: segment of trajectories from individual swimmers colored by time; the short white lines indicate the bacterium's instantaneous swimming orientation. The scale bars in the insets are 2 µm.

References

Nicholas G. Chisholm and Kathleen J. Stebe. Driven and active colloids at fluid interfaces. *Journal of Fluid Mechanics*, 914:A29, May 2021. ISSN 0022-1120, 1469-7645. doi: 10.1017/jfm.2020.708. URL https://www.cambridge.org/core/product/identifier/S0022112020007089/type/journal_article.

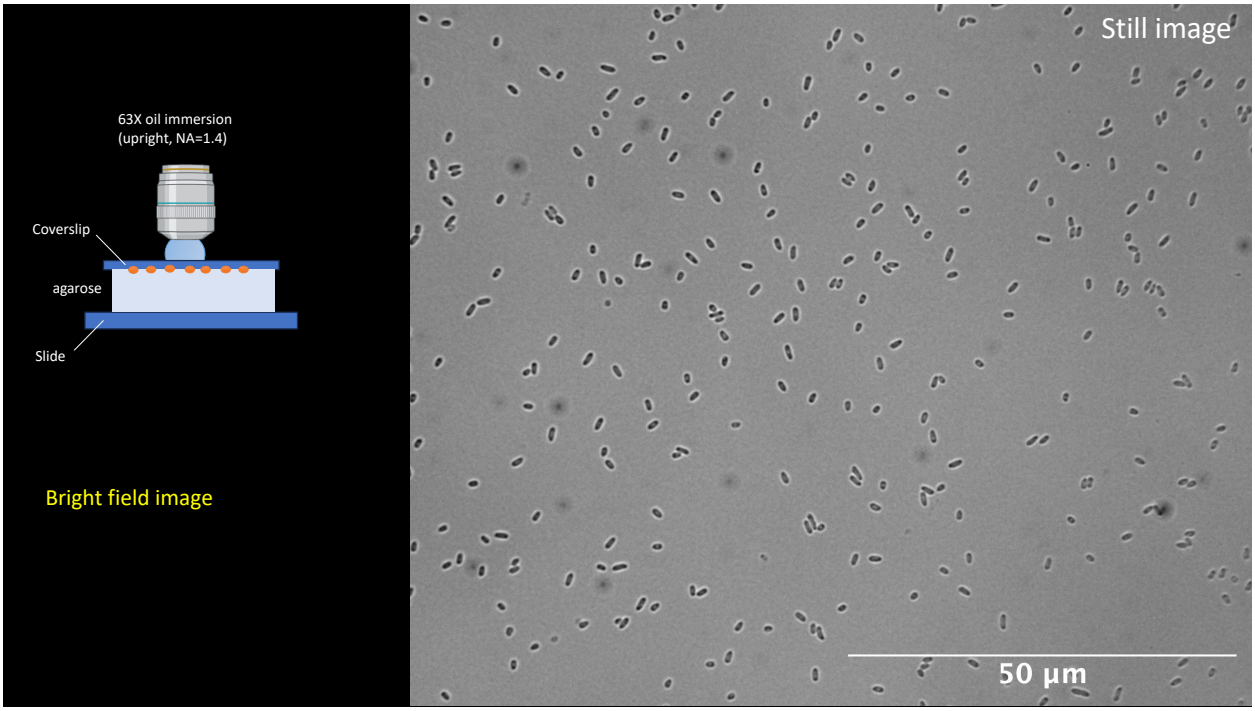

Figure S4: *P.aeruginosa* PA01 cell bodies on agarose gel High resolution bright field images of the PA01 bacterium on an agarose surface are acquired using a 63x oil immersion lens with NA= 1.4. The diffraction limited resolution of this imaging system is $\sim 0.2\,\mu$m.

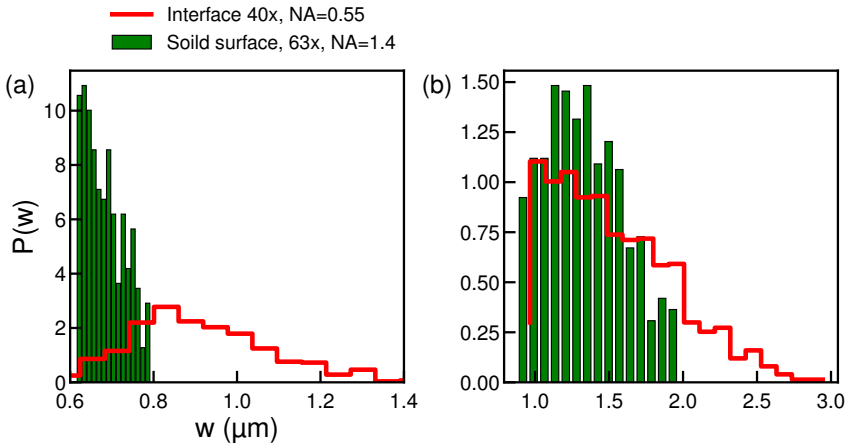

Figure S5: P.aeruginosa cell body and apparent size. Measured width (a) and length (b) of bacteria on solid surface and interface. Green bars: bacteria on agarose surface imaged with 63x oil objective with NA=1.4; red line: bacteria trapped on interfaces imaged with 40x air objective with NA=0.55.

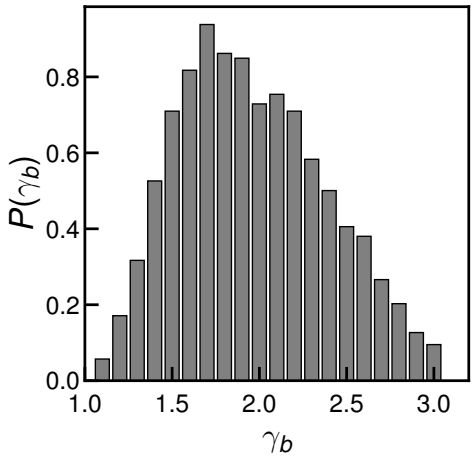

Figure S6: Distribution of aspect ratio of P.aeruginosa. Bacteria are imaged on agarose surface with 63x oil objective with NA=1.4.

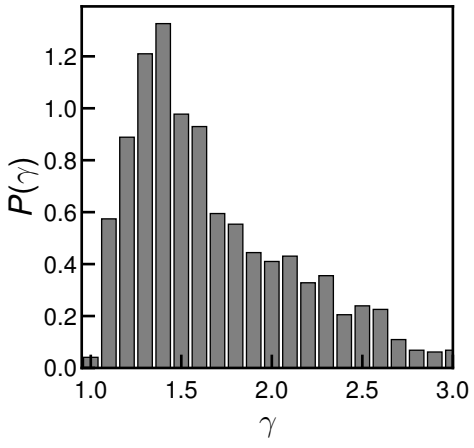

Figure S7: Distribution of apparent aspect ratio of P.aeruginosa. Apparent aspect ratio of bacteria trapped on interfaces imaged with 40x air objective with NA=0.55.